



Contents lists available at ScienceDirect

## Saudi Pharmaceutical Journal

journal homepage: [www.sciencedirect.com](http://www.sciencedirect.com)

Original article

# A preparation technology of volatile components in Linggui Zhugan decoction based on the transfer of cinnamaldehyde and its anti-gastric ulcer effect

Ling Li<sup>a,b</sup>, Nan Wang<sup>b</sup>, Xiaolong Fan<sup>b</sup>, Ning He<sup>a,\*</sup>, Tong Zhang<sup>b,\*</sup><sup>a</sup> College of Pharmacy, Anhui University of Chinese Medicine, Hefei 230000, China<sup>b</sup> School of Pharmacy, Shanghai University of Traditional Chinese Medicine, Shanghai 201203, China

## ARTICLE INFO

## Keywords:

Linggui Zhugan  
Volatile components  
Cinnamaldehyde  
 $\beta$ -cyclodextrin  
Gastric ulcer

## ABSTRACT

**Purpose:** This study aims to preserve the volatile components of Linggui Zhugan (LGZG) decoction, offering an experimental foundation for subsequent preparations efforts.

**Methods:** Two modern sample preparation processes were compared with the traditional method approach using HPLC fingerprints. After identifying the main volatile components in LGZG aqueous decoction, the inclusion method of inclusion compounds (IC-LGZG) was established and optimized at laboratory, pilot and production scales. Characterization, stability testing of IC-LGZG, and experiments on gastric ulcer rats were conducted to validate the transferability of chemical composition and pharmaceutical efficacy.

**Results:** The study focused on preserving the volatile components in LGZG modern preparations. HPLC analysis revealed cinnamaldehyde (CA) as the main volatile component in LGZG decoction. The optimized IC-LGZG preparation involved heating aromatic water to 40 °C, adding 20 g/L of  $\beta$ -Cyclodextrin ( $\beta$ -CD), keeping warm and stirring at 300 r for 30 min. This process exhibited good repeatability across different verification tests at varying scales. IC-LGZG obtained effectively transferred CA molecules into the  $\beta$ -CD molecules via encapsulation, remaining stable when stored in sealed and dark conditions. Finally, CA, IC-LGZG and M-LGZG (a mixture of IC-LGZG and water-soluble extract powder) effectively prevented the formation of gastric ulcer by mitigating reductions in IL-10, SOD and the increase of TNF- $\alpha$ , NO, MDA in serum.

**Conclusion:** The IC-LGZG prepared using this process successfully transfers volatile components, both chemically and pharmacologically, making it suitable for modern preparations of LGZG.

## 1. Introduction

Linggui Zhugan (LGZG), originating from *Synopsis of Prescriptions of the Golden Chamber* written by Zhang Zhongjing during the Han Dynasty (Zhang 2006), was a classic prescription with curative effect that has been inherited for thousands of years in China. It comprises Poria (Pr), Cinnamomi Ramulus (CR), Atractylodis Macrocephalae Rhizoma (AMR) and Glycyrrhizae Radix Et Rhizoma (GRER). However, the traditional preparation method of LGZG has some drawbacks, including its large volume, bitter taste, inconvenience in consumption and portability, susceptibility to mildew and fermentation, and limited shelf life. Transforming LGZG decoction into a contemporary Chinese medicine

preparation that is safe, effective, and quality-controlled has become an urgent to address, which this study aims to resolve. In the prescription, both CR and AMR both contain volatile components with medicinal effects. The main active component of CR is its volatile oil, which is about 1% (Liu et al., 2013), known for its anti-inflammatory, antiviral, antitumor and antibacterial effects (Xu et al., 2016, Liu et al., 2020, Jia et al., 2023). The volatile oil in LGZG decoction contributes significantly to its actions, such as warming yang and transforming water retention, strengthening the spleen and harmonizing the stomach. These effects are considered crucial in treating water stagnancy led by deficiency of middle Yang. Previous studies have indicated that volatile components in traditional Chinese medicine or prescriptions can be retained after

Peer review under responsibility of King Saud University.

\* Corresponding authors.

E-mail addresses: [liling\\_sh@163.com](mailto:liling_sh@163.com) (L. Li), [w\\_nan8797@163.com](mailto:w_nan8797@163.com) (N. Wang), [2447756953@qq.com](mailto:2447756953@qq.com) (X. Fan), [hening826@163.com](mailto:hening826@163.com) (N. He), [zhangtong@shutcm.edu.cn](mailto:zhangtong@shutcm.edu.cn) (T. Zhang).

<https://doi.org/10.1016/j.jsps.2023.101833>

Received 21 August 2023; Accepted 15 October 2023

Available online 19 October 2023

1319-0164/© 2023 The Author(s). Published by Elsevier B.V. on behalf of King Saud University. This is an open access article under the CC BY-NC-ND license (<http://creativecommons.org/licenses/by-nc-nd/4.0/>).

being prepared by traditional decoction (Luo et al., 2016, Li et al., 2022). Therefore, retaining volatile components in LGZG decoction is necessary. However, the prevalent industrial preparation processes, including reflux extraction, concentration, drying, pulverization, are not conducive to the retention of heat-unstable components, especially volatile ones. Therefore, the decision to preserve these volatile components should be based on the consistency of samples obtained from traditional and modern preparation processes.

The first step is to extract the volatile components. The extraction methods include steam distillation method, solvent method, microwave method, ultrasonic method, supercritical fluid extraction method and so on. Steam distillation is the most used method in industry because of its simple equipment and low cost (Cheng et al., 2022). Retaining these volatile components is another crucial step, accomplished through methods like cyclodextrin inclusion technology, solidified adsorption and treated with micro emulsification, microencapsulation or micro spherization (Wang et al., 2022). Among these, cyclodextrin inclusion technology stands out as a commonly used method. Previous studies have used cyclodextrin inclusion to enhance the active components stability and efficacy in vivo (Su et al., 2019, Jiang et al., 2022, Niu 2022). However, the mixed volatile oil of CR and AMR was found to have a similar density to water, leading to poor separation effect of oil-water and the formation of insoluble white flocculents (Gu et al., 2019). Some studies attempted secondary distillation of aromatic water to extract volatile oil (Li et al., 2016, Xiang et al., 2017). However, this method is complex and time consuming, hindering subsequent equipment scaling. Consequently, this research utilized aromatic water instead of volatile oil.

In terms of the clinical application of LGZG decoction, Zhang Yu and other scholars (Zhang 2019) studied more than 300 medical cases on epigastric and abdominal pain recorded by famous masters before the end of the Qing Dynasty (1911), and pointed out that LGZG decoction was one of the six most commonly used prescriptions for treating stomach-ache. In modern clinical application, the same medication pattern has also been found, and LGZG is often used as a basic prescription in the clinical treatment of epigastric pain, with better curative effect (Zhang et al., 2011, Wang 2012, Ye 2016, Xie 2017). Gastric ulcer models, particularly those induced by ethanol, mimic clinical features and are commonly used in to establish rat studies (Badr et al., 2023, Zhao et al., 2023).

In this study, the necessity of retaining volatile components in LGZG decoction was further determined based on the samples prepared by the traditional decocting method. Aromatic waters from the LGZG extraction, containing volatiles components, were analyzed via high-performance liquid chromatography (HPLC), to identify major components. The HPLC method for the main ingredient was established to study the technological parameters of the inclusion of  $\beta$ -Cyclodextrin ( $\beta$ -CD) and aromatic water, forming the inclusion compound-LGZG (IC-LGZG). IC-LGZG was then characterized and identified by HPLC, Thin Layer Chromatography (TLC) and Fourier Transform Infrared Spectroscopy (FT-IR), and its stability was accessed under various conditions to ensure the retention of volatile components and preservation condition of IC-LGZG. Subsequently, SD rats were administered IC-LGZG and related solutions to verify its efficacy on the ethanol-induced gastric ulcer model. Inflammatory and oxidative factors in the serum were analyzed to study the mechanism of IC-LGZG against gastric ulcer. This study aimed to confirm that the IC-LGZG preparation method preserved LGZG decoction's volatile, ensuring its pharmacodynamic effects and maintaining consistency between traditional and modern preparations.

## 2. Materials and methods

### 2.1. Materials

Cinnamaldehyde (CA, purity was 99.6 %) was purchased from Chinese Institute for Food and Drug Control. China National Medicines Co.,

Ltd. (Shanghai, China) provided methanol (MeOH), ethanol (EtOH),  $\beta$ -Cyclodextrin, phosphoric acid and acetonitrile (chromatographic grade, Thermo Fisher Scientific, MA, USA). Water was generated from a Milli-Q academic system (Millipore, USA). Poria, Cinnamomi Ramulus, Atractylodis Macrocephalae Rhizoma, Glycyrrhizae Radix Et Rhizoma were purchased from Jiangsu Sanhe Xing Chinese Medicine Research Co., Ltd. (Lianyungang, China), and were identified as authentic by Associate Professor Zhang Hongmei of Shanghai University of Traditional Chinese Medicine. M-LGZG (the mixture of IC-LGZG and water-soluble extract powder) was made in laboratory (No. 202009-1). Aromatic water was obtained during the extraction of LGZG.

### 2.2. Comparison of different preparation methods of LGZG

#### 2.2.1. Preparation of LGZG with different methods

Traditional preparation method (Fig. 1A(a)): Pr, CR, AMR, GRER were taken with single prescription by adding 1200 mL pure water and then soaked for 30 min. The mixture was heated until the decoction's volume reached 600 mL, and the samples named TP-LGZG was obtained by liquid medicine freeze-drying.

Modern technological preparation method (Fig. 1A(b)): Pr, CR, AMR, GRER were taken with specific proportion, adding 10 times the amount of pure water, and soaked for 30 min, heating and refluxing twice. The extracted liquid was concentrated to a certain volume (60 °C), dried under vacuum (60 °C), and then the dry extract was crushed to obtain a water-soluble extract powder, which called MP-LGZG.

Dual extract method (Fig. 1A(c)): Referring to the method of MP-LGZG, connect the volatile component receiving device to collect water-soluble components and volatile components at the same time.

#### 2.2.2. HPLC fingerprint analysis

2.2.2.1. *Sample preparation.* Accurately weigh 4 g of TP-LGZG and MP-LGZG in two conical bottles respectively, add 10 mL 50 % methanol, and weigh them again. After sonication for 30 min, the samples were weighed after cooling, and the lost weight was added up with 50 % methanol. After shaking, the sample solution was obtained after passing through 0.45  $\mu$ m filter membrane. 5 mL aromatic water was put into a 10 mL volumetric bottle, filled with methanol, mixed, and then filtered through 0.45  $\mu$ m microporous membrane to obtain aromatic water sample.

Analysis was performed on an HPLC system (1260, Agilent, USA) with an Welchrom C18 (4.6 mm  $\times$  250 mm, 5  $\mu$ m) column, using a gradient elution of 0.05 % phosphoric acid water (A) and acetonitrile (0 ~ 50 min, 95 % ~ 40 %A; 50 ~ 60 min, 40 % ~ 0%A; 60 ~ 61 min, 0 % ~ 95 %A; 61 ~ 65 min, 95 %A) at a flow rate of 1.0 mL/min. Column temperature was 25 °C, with a detection wavelength of 220 nm. The injection volume is 10  $\mu$ L (Gu 2020).

### 2.3. Optimization of preparation of IC-LGZG

#### 2.3.1. Cinnamaldehyde (CA) content determination by HPLC

2.3.1.1. *Sample preparation.* 0.01 g IC-LGZG was accurately weighed and placed in a conical flask with a tight-fitting plug, and 50 mL 70 % ethanol was added precisely. The weight was weighed before and after ultrasonic extraction for 30 min. After cooling, the lost weight was made up with 70 % ethanol and filtered through a 0.45  $\mu$ m microporous filter membrane.

2.3.1.2. *Method of HPLC.* Determination was performed on an HPLC system (1260, Agilent, USA) with a Welchrom C18 (4.6 mm  $\times$  250 mm, 5  $\mu$ m) column, using acetonitrile-0.05 % phosphoric acid water (38:62) at a flow rate of 1.0 mL/min. Column temperature was 25 °C, with a detection wavelength of 290 nm and an injection volume of 10  $\mu$ L. The

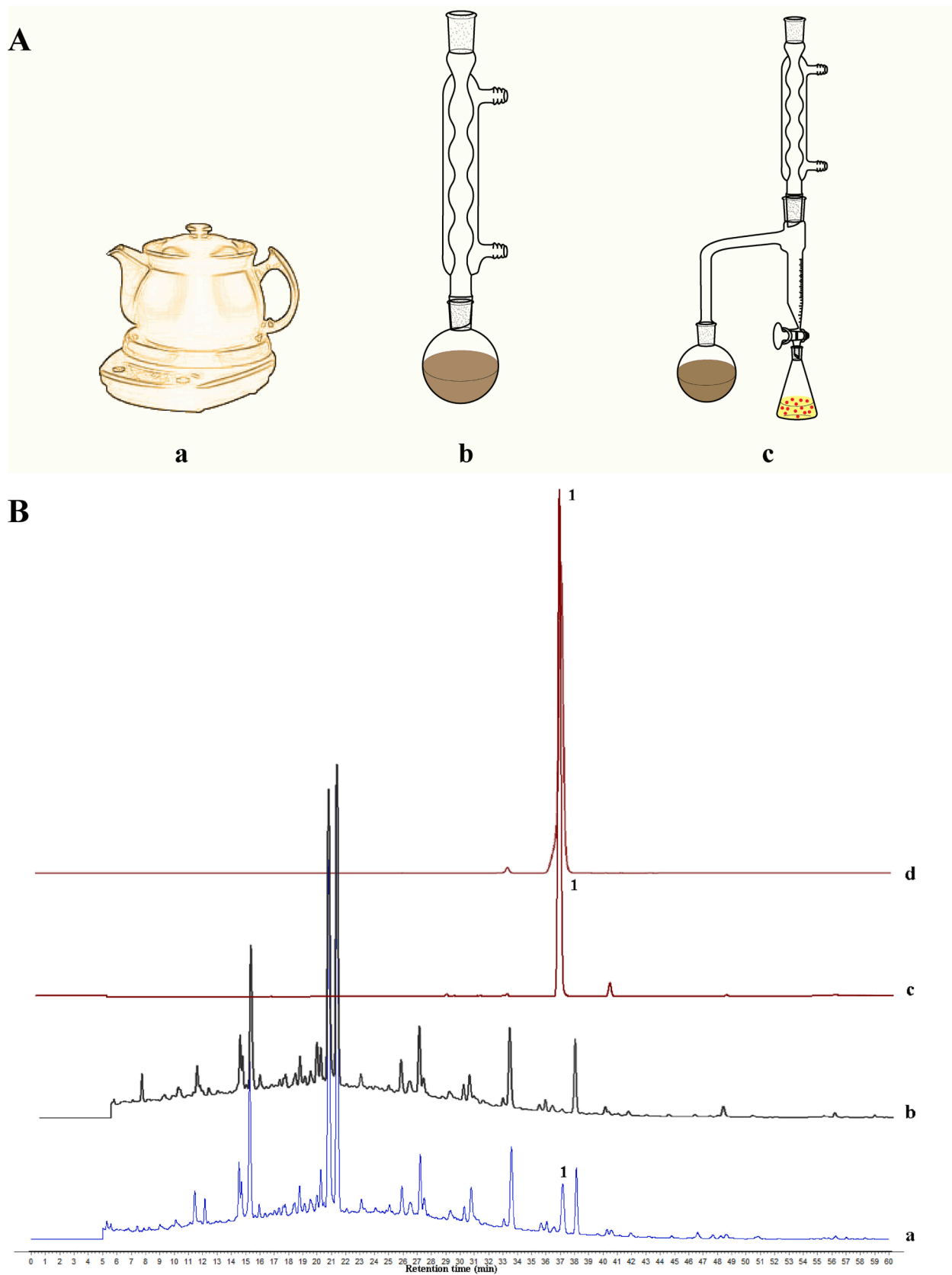


**Fig. 1.** Device diagram of different extraction methods (A): a. Traditional preparation method; b. Modern technology preparation method; c. Double extract method. The fingerprint chromatogram (B) of TP-LGZG (a), MP-LGZG (b), Aromatic water (c), CA (d), 1. CA.

IC-LGZG content of CA was reported as the average drug content ( $n = 3$ ). The content of CA in IC-LGZG and the inclusion rate were calculated, and the formula for the inclusion rate was as follows Eq. (1).

$$\text{Inclusion rate(\%)} = \frac{\text{CA content in IC-LGZG (mg/g)} \times \text{Amount of IC-LGZG (g)}}{\text{CA content in aromatic water (mg)}} \times 100\% \quad (1)$$

**2.3.1.3. Validation of the HPLC method.** CA was accurately weighed and a series of reference solutions (8.19, 16.38, 32.76, 65.52, 131.04  $\mu\text{g/ml}$ ) were prepared, and then analysed by HPLC. The standard curve was established with the concentration as the horizontal coordinate and the peak area as the vertical coordinate. The precision was evaluated with the same samples (IC-LGZG, reference solution) six times. Stability tests were performed at 0, 2, 4, 6, 8, 10, 12 and 24 h using the same IC-LGZG sample solution. In addition, repeatability was measured by preparing 6 sample solutions in parallel with the same IC-LGZG powder. Sample recovery inspection test: 5 mg IC-LGZG was precisely weighed, and the corresponding 50 %, 100 % and 150 % CA were added respectively. The following methods were the same as 'Sample preparation', and each sample was prepared in parallel 3 times.

#### 2.3.2. Concentrations of $\beta$ -CD

Adding  $\beta$ -CD makes aromatic aqueous solution to form a saturated solution at room temperature, and then add  $\beta$ -CD with 8 times, 10 times and 12 times the content of CA in aromatic water. The mixture was stirred at 40 °C for 1 h, left at 4 °C for 24 h and then filtered. The IC-LGZG was obtained after precipitate dried at 40 °C.

#### 2.3.3. Orthogonal optimization

The content of CA in the IC-LGZG was taken as the index of investigation. The main factors included inclusion temperature (40 °C, 50 °C, 60 °C), stirring rate (200 r, 300 r, 400 r) and inclusion time (30 min, 45 min, 60 min). The experiment follows  $L_9(3^4)$  orthogonal experimental design.

$$\text{Overall score} = \frac{\text{CA content}}{\text{Highest CA content}} \times 100 \quad (2)$$

#### 2.3.4. Drying temperature

A certain amount of aromatic water was used for inclusion and washing according to the preferred encapsulation process. Then they were dried at 40 °C, 50 °C and 60 °C, respectively, pulverized and the content of CA in the IC-LGZG was determined, and the inclusion rate was calculated.

#### 2.3.5. Demonstration test

The inclusion of aromatic water was carried out by the above optimal process, and the validation experiment was carried out at laboratory, pilot, and production scales. And the content of CA in IC-LGZG was also determined.

### 2.4. Characterization analysis of IC-LGZG

#### 2.4.1. HPLC fingerprint and component attribution

Samples for HPLC fingerprint analysis were prepared by taking 0.05 g of IC-LGZG, 4 g of M-LGZG (the mixture of IC-LGZG and water-soluble extract powder). Meanwhile, reference solutions were injected into HPLC for analysis. The method of sample preparation and HPLC were same with "2.2.2.2". The similarity between M-LGZG and TP-LGZG was

analyzed by the "Similarity Evaluation System of TCM Chromatographic Fingerprints".

#### 2.4.2. TLC

To verify whether the volatile components in aromatic water are encapsulated in  $\beta$ -CD, TLC method was used to detect. Some test sample solutions were prepared.

**Sample a:** aromatic water was stirred with petroleum ether, and the supernatant was taken to obtain.

**Sample b:** a certain amount of IC-LGZG was weighed and shaken by adding petroleum ether. After standing, the supernatant was taken to obtain.

**Sample c:** a certain amount of IC-LGZG was weighed and de-inclusion was carried out by ultrasound in 70 % methanol to obtain.

**Sample d:** a certain amount of  $\beta$ -CD was weighed and shaken with petroleum ether, and the supernatant was taken after standing to obtain negative test.

**Sample e:** a certain amount of CA and  $\beta$ -CD were taken, mixed evenly, and then shaken with petroleum ether, the supernatant was obtained.

2  $\mu\text{L}$  of each of the above five test sample solutions were absorbed by capillary tube and placed on the same silica gel G thin-layer plate. Using ethyl acetate: petroleum ether (60 ~ 90 °C) (3:17) as the development agent, the thin layer plate was expanded, removed, dried, and sprayed with dinitrophenylhydrazine ethanol test solution.

#### 2.4.3. FT-IR

Appropriate amounts of CA,  $\beta$ -CD, IC-LGZG, and the physical mixture of CA and  $\beta$ -CD were taken, and the samples were pressed with potassium bromide to determine the infrared spectrogram by Fourier transform infrared spectrometer (Thermo Fisher Scientific, USA).

### 2.5. Stability of IC-LGZG

To investigate the factors affecting the stability of the product and the storage conditions of IC-LGZG, IC-LGZG with sealed and open state, with a CA content of 75.170 mg/g, were exposed to high temperature conditions at 40 °C and 60 °C, a strong light environment (4500 lx  $\pm$  500 lx) respectively. After 10 days, the CA content in IC-LGZG after placement for each condition was determined.

### 2.6. Anti-ulcer effect of IC-LGZG

#### 2.6.1. Animal groups

Sprague Dawley (SD, 6–8 weeks) rats were purchased from B&K Universal Group Limited. All rats were kept in specific pathogen-free (SPF) barrier conditions with temperature-controlled room (22–24 °C), and were housed in standard rat cages with ad libitum access to water and food for one week before the experimentation. All animal care and experimental protocols were performed under Shanghai University of Traditional Chinese Medicine Institutional Animal Care and Use Committee (IACUC). The rats were randomly assigned to the following groups ( $n = 6$  each): Control group (0.25 % Na-CMC and 0.5 % Tween-80), EtOH group (0.25 % Na-CMC and 0.5 % Tween-80), CA treated group (40 mg/kg), IC-LGZG treated group (100 mg/kg, provided by Jiangsu Kanion Pharmaceutical Co., LTD. No. Z201101), M-LGZG treated group (600 mg/kg), Ranitidine treated group (40 mg/kg). The

CA, IC-LGZG, M-LGZG and Ranitidine groups were orally administered pre-treatments from days 1–7. On day 7, all rats except those in the control group were orally administered with ethanol (5 mL/kg bw) after 30 min of treatment. Two hours after ethanol treatment, all rats were sacrificed. And the stomachs and blood samples were collected for further studies.

### 2.6.2. Assessment of gastric mucosal injury

The stomach of rats was photographed, and Image-Pro Plus 6.0 software was used to calculate the area of GU and the total area of the stomach of each rat, and calculating the ratio of ulcer area.

$$\text{Ulcer area ratio (\%)} = \frac{\text{Ulcer area}}{\text{Total area of stomach}} \times 100\% \quad (3)$$

### 2.6.3. Histopathological evaluation

Gastric tissue was fixed with 4 % paraformaldehyde, embedded in paraffin, and cut at a thickness of 5  $\mu\text{m}$  and stained with Haematoxylin–Eosin (H&E). Each section was observed by using an Olympus IX83 microscope (Tokyo, Japan). The histopathological scores with each group were calculated according to Table 1 (Li et al., 2022).

### 2.6.4. Estimation of serum biochemical parameters

Serum samples were collected after blood samples standing and centrifuging to assess biochemical parameters. The levels of SOD and MDA in serum were assessed by commercial assay kits. Rat cytokines such as TNF- $\alpha$ , IL-10, and NO in serum were determined using ELISA kits. All procedures were carried out according to the manufacturer's protocols.

### 2.6.5. Statistical analyses

Data are indicated by mean values  $\pm$  SD. Statistical significance was evaluated with Student's *t*-test or ANOVA test followed by Tukey's multiple comparison test (GraphPad Prism 8.0). Statistical significance is expressed with \* $p < 0.05$ , \*\* $p < 0.01$ , \*\*\* $p < 0.001$ , \*\*\*\* $p < 0.0001$ .

## 3. Results

### 3.1. Difference of LGZG obtained by different preparation methods

As can be seen from the Fig. 1B, water-soluble extract powder (b) prepared by the modern technique lacked the peak with a retention time of 37 min in the fingerprint spectrum, compared with TP-LGZG (a) prepared by traditional method. According to the comparison, the component corresponding to this peak is the volatile component CA,

**Table 1**  
Rules of scoring with histopathological.

Score	Gastric mucosal oedema	Leukocytes infiltration	Gastric haemorrhage	Gastric mucosal injury
0	Absent	Absent	Absent	Intact
1	Gentle	<10 % of total area/LPF	1–10/HPF	Desquamation of epithelial lamina
2	Moderate	11–20 % of total area/LPF	11–20/HPF	Desquamation of superficial lamina propria or 1/3 reduction of gastric glands
3	Grievous	21–30 % of total area/LPF	21–30/HPF	Desquamation of middle lamina propria or 2/3 reduction of gastric glands
4	/	>30 %	>30/HPF	Desquamation of lower lamina propria or > 2/3 reduction of gastric glands, even exposure of submucosa

which came from CR. The analysis of the composition of aromatic water collected by dual extraction method shows that its main component is CA, which can make up for the deficiency of CA in water-soluble extract powder. Therefore, more attention should be given to the retention of volatile components when transforming LGZG into modern preparations.

### 3.2. Methodological investigation of CA content determination in IC-LGZG

The determination of CA content in IC-LGZG showed good linearity between the concentration of 8.19–131.04  $\mu\text{g/ml}$  ( $y = 107.15x + 8.2164$ ,  $r = 0.9999$ ), and the precision of samples and reference samples was good, with RSD of 0.09 % and 0.42 %, respectively. The sample preparation method was reproducible, and the prepared sample solution was stable within 24 h. The accuracy of sample preparation was good, and the recovery rates of low, medium, and high samples were 96.63 %, 97.60 %, 102.57 % (RSD = 2.85 %), respectively.

### 3.3. Preparation technology of IC-LGZG

#### 3.3.1. Times the dosage of $\beta$ -CD

Investigation results of  $\beta$ -CD dosage was shown in Table 2. There appeared to be no significant difference in the content and encapsulation rate in IC-LGZG when 8, 10 and 12 times of CA content was added in aromatic water. It is calculated that the mass of 8 times the amount of  $\beta$ -CD used to the volume of aromatic water was 50:1. The final dosage of  $\beta$ -CD was 20 g/L aromatic water.

#### 3.3.2. Orthogonal optimization

The direct analysis result (Table 3) showed that the primary and secondary relationship of the three factors is  $A > B > C$ , and the optimal process is  $A_3B_2C_1$ . Since the sum of squared deviations of terms B and C is less than the error term, B and C are incorporated into the error term for calculation. The result of variance analysis (Table 4) shows that the sum of squared deviations of the three terms are very small, and there is no significant difference. The optimal process is  $A_1B_2C_1$  according to the actual production conditions. All in all, the chosen method of inclusion was: inclusion temperature at 40  $^{\circ}\text{C}$ , 300r for the rotation speed, and 30 min for the inclusion time.

#### 3.3.3. Drying temperature

The results showed that the inclusion rate of CA decreased with increasing temperature (Table 5), indicating that the drying temperature influenced the inclusion complex. Therefore, 40  $^{\circ}\text{C}$  was chosen to be the drying temperature of IC-LGZG.

#### 3.3.4. Process validation

The final selection of inclusion method: Heating aromatic water to 40  $^{\circ}\text{C}$ , then adding 20 g/L of  $\beta$ -CD, keeping it warm and stirring at 300 r/min for 30 min. After stirring, the mixture was placed at 4  $^{\circ}\text{C}$  for 24 h and then filtered. The filter residue was rinsed with saturated aqueous solution of  $\beta$ -CD, and the inclusion precipitate was collected, dried at 40  $^{\circ}\text{C}$ , and ground into powder to obtain IC-LGZG.

The experimental results (Table 6) showed that the content of CA in IC-LGZG prepared by this method in laboratory scale was 79.82 mg/g (RSD = 0.88 %), which in pilot scale was 86.32 mg/g (RSD = 1.28 %), in production scale was 90.48 mg/g (RSD = 0.60 %). And the RSD of CA

**Table 2**  
The results of the amount of  $\beta$ -CD ( $n = 2$ ).

Different times	CA content (mg/g)	inclusion rate /%
8 times	86.448	61.80
10 times	86.021	60.86
12 times	86.112	64.91

**Table 3**  
Experimental results of orthogonal design.

No.	Experimental factor and level				CA content (mg/g)	Overall score
	Inclusion temperature	Stirring rate	Inclusion time	Error		
1	1	1	1	1	84.944	98.61
2	1	2	2	2	84.993	98.66
3	1	3	3	3	84.440	98.02
4	2	1	2	3	84.446	98.03
5	2	2	3	1	85.255	98.97
6	2	3	1	2	85.157	98.86
7	3	1	3	2	84.758	98.39
8	3	2	1	3	85.583	99.35
9	3	3	2	1	86.143	100
K1	98.430	98.343	98.940	99.193		
K2	98.620	98.993	98.897	98.637		
K3	99.247	98.960	98.460	98.467		
Range	0.817	0.650	0.480	0.726		

**Table 4**  
Analysis of variance.

Factors	SS	df	F	F critical value	Significance
inclusion temperature	1.096	2	1.570	5.14	P > 0.05
stirring rate	0.804	2	1.152	5.14	P > 0.05
inclusion time	0.423	2	0.606	5.14	P > 0.05
error	2.094	6			

**Table 5**  
Investigation of drying temperature (n = 2).

Different temperature	Inclusion rate (%)
40 °C	55.08
50 °C	42.68
60 °C	39.59

content in IC-LGZG of three scales was 5.50 %, indicating that the inclusion process is stable.

### 3.4. Characterization of IC-LGZG

#### 3.4.1. HPLC fingerprint

As can be seen from the Fig. 2A, five components were found in aromatic water were identified, containing namely Coumarin (peak 1), Cinnamic acid (peak 2), CA (peak 3) and 2-methoxy cinnamaldehyde (peak 4) and Atractylenolide III (peak 5). All the components were transferred to the IC-LGZG after the aromatic water passes through the inclusion. After mixing IC-LGZG with water-soluble extract powder, the corresponding peaks of CA could be seen in the HPLC chromatogram of M-LGZG, and the similarity between M-LGZG and TP-LGZG was 0.995.

#### 3.4.2. TLC

As can be seen from the Fig. 2B, samples a (supernatant of aromatic water), c (de-inclusion solution) and e (physical mixture of  $\beta$ -CD and CA) showed yellow spots at the same position. Samples b (supernatant of IC-LGZG) and d ( $\beta$ -CD) had no spots at the corresponding position, indicating that there was no CA residue on the surface of the inclusion complex. The properties of the inclusion complex did not change during the inclusion process, and CA entered the  $\beta$ -CD molecule.

#### 3.4.3. FT-IR

In the infrared spectrum (Fig. 2C), the strong absorption peak of the  $\beta$ -CD (a) at 3404.76  $\text{cm}^{-1}$ , the strong absorption peak of the physical mixture of  $\beta$ -CD and CA (c) at 3393.97  $\text{cm}^{-1}$ , and the strong absorption peak of the IC-LGZG (b) at 3361.97  $\text{cm}^{-1}$  moved to the low wave number direction obviously. CA (d) had a strong absorption peak at 1678.01  $\text{cm}^{-1}$ , and the absorption peak was significantly shifted at 1669.89  $\text{cm}^{-1}$

**Table 6**  
Validation of experimental results (n = 3).

Scale	No.	CA content (mg/g)	Average (mg/g)	RSD
Laboratory	1	79.12	79.82	0.88 %
	2	80.53		
	3	79.82		
Pilot	1	86.61	86.32	1.28 %
	2	87.25		
	3	85.10		
Production	1	90.07	90.48	0.60 %
	2	90.28		
	3	91.09		
RSD		5.50 %		/

after inclusion of  $\beta$ -CD (b). All of them were obviously different from the physical mixture (c), indicating that CA had formed inclusion complex with  $\beta$ -CD.

### 3.5. Stability of IC-LGZG

High temperature and strong light have a great effect on the CA content in IC-LGZG when it is not sealed in an aluminum foil pouch (Qiang et al., 2014). After sealed packaging, the CA content did not change much at 40 °C and 60 °C, but increased significantly under the condition of strong light (Fig. 2D). The content of CA is more stable with sealed than un-sealed. Therefore, IC-LGZG should be sealed and stored away from light after preparation.

### 3.6. Anti-ulcer effect of IC-LGZG and M-LGZG

#### 3.6.1. Mucosal damage in rat

The ulcer area ratio was assessed in the ethanol-induced group of rats. The morphology of gastric tissue (Fig. 3A) clearly showed that the gastric mucosa of control group was normal, smooth and undamaged, whereas that of EtOH group had many obvious bleeding points and erosions. The gastric mucosal injury was remarkably ameliorated in all drug-treated group, which was consistent with the results of the ulcer area ratio (Fig. 3B). Among them, the CA and IC-LGZG groups had a lower degree of ulceration and almost no ulcer manifestations were observed ( $p < 0.0001$ ). M-LGZG group and Ranitidine group also effectively prevented the formation of gastric ulcer ( $p < 0.05$ ,  $p < 0.001$ ).

Examination on H&E-stained sections showed that EtOH-induced ulcer exhibited notable damages in gastric mucosal structure with extensive infiltration of inflammatory cells, along with erosion, haemorrhage, oedema, mucosa cells depletion (Fig. 4A). The score of H&E pathological section (Fig. 4B) was consistent with the apparent ulcer area, which the score of the administration group was significantly different from that of the Model group. It shows that the inclusion of CA does not affect its anti-gastric ulcer effect, it also exerted its anti-gastric

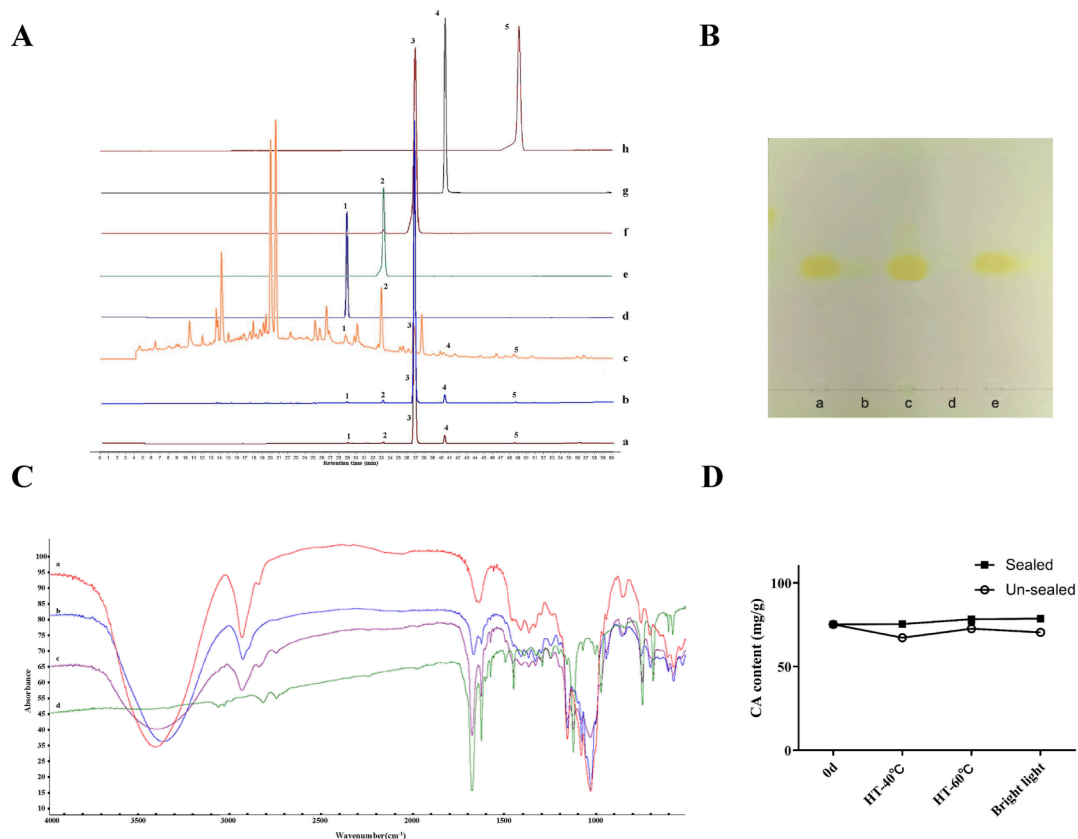


**Fig. 2.** Characterization and stability of IC-LGZG. (A) HPLC fingerprint of Aromatic water (a), IC-LGZG (b), M-LGZG (c), Coumarin (d), Cinnamic acid (e), CA (f) and 2-methoxy cinnamaldehyde (g) and Atractylenolide III (h). 1. Coumarin, 2. Cinnamic acid, 3. CA, 4. 2-methoxy cinnamaldehyde, 5. Atractylenolide III; (B) TLC of supernatant of aromatic water (a), supernatant of IC-LGZG (b), de-inclusion solution (c), supernatant of  $\beta$ -CD (d), supernatant of CA and  $\beta$ -CD physical mixture (e); (C) The results of FT-IR with  $\beta$ -CD (a), IC-LGZG (b), CA and  $\beta$ -CD physical mixture (c), CA (d); (D) Stability of IC-LGZG, Data are expressed as mean  $\pm$  SD (n = 3).

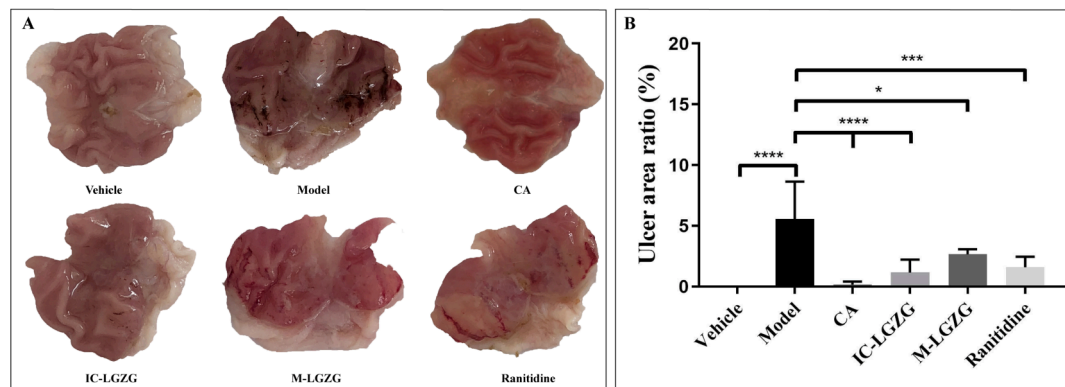


**Fig. 3.** Apparent gastric tissue morphology of rats in each group (A) and Ulcer area ratio (B). Data are expressed as mean  $\pm$  SD (n = 6), \* $p$  < 0.05, \*\*\* $p$  < 0.001, \*\*\*\* $p$  < 0.0001 vs Model group.

ulcer effect when mixed with extract powder.

### 3.6.2. The levels of inflammation and oxidative stress in the serum

The inflammatory factors and oxidation indexes in serum of rats were detected. Inflammation is an inevitable response in ethanol-induced gastric ulcer. A variety of mediators also changed during this process. EtOH significantly decreased anti-inflammatory cytokine IL-10 in the serum ( $p$  < 0.0001, Fig. 5A) and increased pro-inflammatory cytokine TNF- $\alpha$  ( $p$  < 0.0001, Fig. 5B), pro-inflammatory mediator NO production in the serum ( $p$  < 0.0001, Fig. 5C) compared to those in the vehicle group. And CA, IC-LGZG, M-LGZG effectively restored IL-10

content ( $p$  < 0.0001,  $p$  < 0.05,  $p$  < 0.0001, Fig. 5A), TNF- $\alpha$  content ( $p$  < 0.0001,  $p$  < 0.001,  $p$  < 0.0001, Fig. 5B) and NO level ( $p$  < 0.0001,  $p$  < 0.001,  $p$  < 0.0001, Fig. 5C).

Compared with vehicle group, the content of SOD shown a significant decrease ( $p$  < 0.0001, Fig. 5D) while MDA increased significantly ( $p$  < 0.0001, Fig. 5E) in model group serum, which indicated enhanced oxidative stress. CA and M-LGZG can amplify the decrease of SOD, compared with model group ( $p$  < 0.0001,  $p$  < 0.001, Fig. 5D). CA, IC-LGZG and M-LGZG can reduce the increase of MDA content effectively ( $p$  < 0.0001,  $p$  < 0.01,  $p$  < 0.05, Fig. 5E).

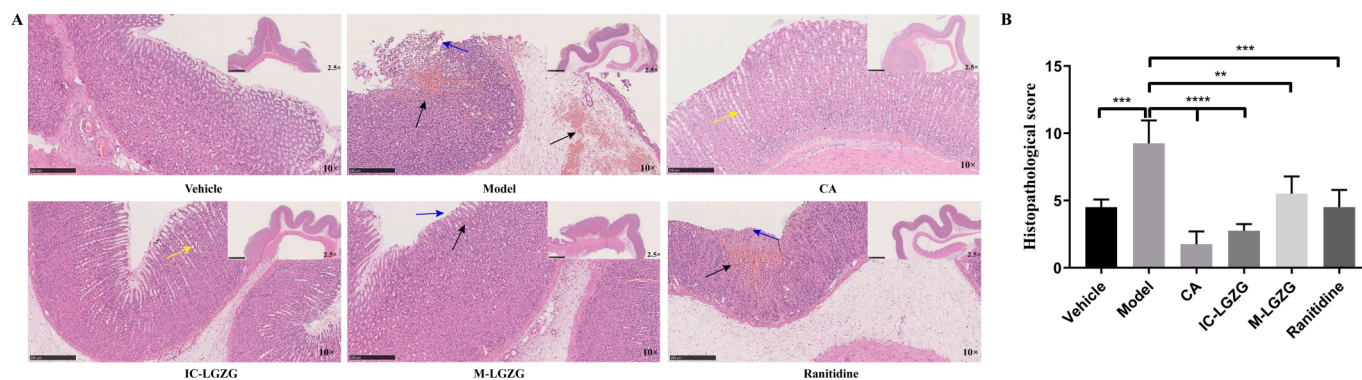


**Fig. 4.** H&E-stained histological sections of rats' gastric tissues in each group (A) and Histopathological scores of gastric tissues (B). Blue arrows indicate mucosal injury, black arrows mark bleeding, and yellow arrows indicate edema. Data are expressed as mean  $\pm$  SD (n = 4), \*\* $p$  < 0.01, \*\*\* $p$  < 0.001, \*\*\*\* $p$  < 0.0001 vs Model group.

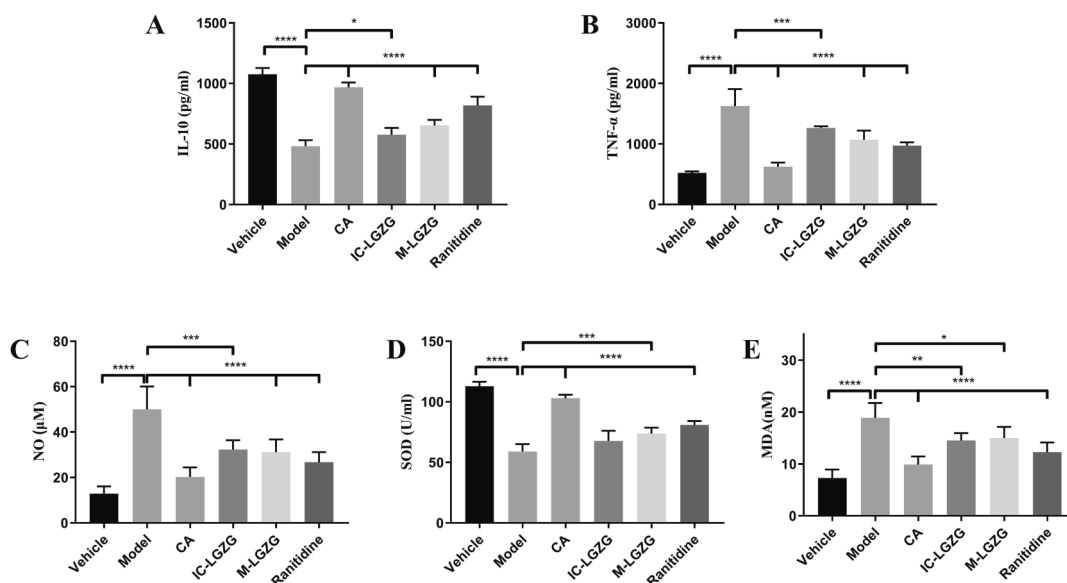


**Fig. 5.** The content of oxidative stress and inflammation in the 6 groups. (A) IL-10; (B) TNF- $\alpha$ ; (C) NO; (D) SOD and (E) MDA. Data are expressed as mean  $\pm$  SD (n = 6). \* $p$  < 0.05, \*\* $p$  < 0.01, \*\*\* $p$  < 0.001, \*\*\*\* $p$  < 0.0001 vs Model group.

#### 4. Discussion

Firstly, the samples prepared by two modern sample preparation methods were compared with those prepared by the traditional method, and their fingerprints chromatograms were analyzed by HPLC. The analysis revealed the presence of the volatile component CA in the traditional decoction, constituting the main volatile components in CR volatile oil. Therefore, a dual extraction method was adopted to capture the volatile components and the subsequent retention process was investigated while extracting the water-soluble components.

The aromatic water components included coumarin, cinnamic acid, CA, 2-methoxy cinnamaldehyde, and atractylenolide III, with CA accounted for 95.61 % of the total peak area of the fingerprint. To obtain stable inclusion complex, the evaluation focused on CA content, and the preparation process for the inclusion complex was optimized. A HPLC method for the determination of CA in IC-LGZG was developed, referencing the 2020 Chinese Pharmacopoeia for CR's CA determination, and the methodology was verified.

Cyclodextrin refer to a series of cyclic oligosaccharides from amylose with the assistance of cyclodextrin glucosyl transferase produced by *Bacillus*. Among these,  $\beta$ -CD has the lowest solubility in water and is the easiest to crystallize from water. It is frequently used in large-scale

modern production due to its abundant supply and economical cost (Yi and Chen 2006). Volatile components can be encapsulated in the molecular pores of  $\beta$ -CD to form molecular capsules. This encapsulation prevents the components from interacting with the external environment, enhancing the stability of the substance, and enabling the transformation of liquid drugs into powder for easier. Common inclusion methods encompass saturated aqueous solution, grinding and ultrasonic techniques (Li et al., 2016, Xiang et al., 2017). In this study, the saturated aqueous solution method, previously reported as the best for incorporating volatile oil mixed with CR and AMR, was employed (Xiang et al., 2017).

The inclusion process involves the binding of  $\beta$ -CD's main molecule to the guest molecule CA through hydrophobic or hydrogen bonding interactions (Xiang et al., 2017).  $\beta$ -CD and CA have relative molecular weights of approximately 1135 and 132, respectively. Most  $\beta$ -CD inclusion complexes maintain 1:1 ratio between host and guest molecules (Christaki et al., 2023, Mic et al., 2023). Considering that the molar mass ratio of  $\beta$ -CD to CA is 8:1, the amount of  $\beta$ -CD added was studied based on an 8-fold CA content in aromatic water. On the other hand, due to the high-water content in aromatic water, most  $\beta$ -CD dissolves during the filtration of IC-LGZG and cannot be recovered. Therefore, an innovative approach was taken by first adding  $\beta$ -CD to form a saturated solution of



aromatic water- $\beta$ -CD at room temperature (18 g/L, 20 °C) (Fu 2008). Subsequently, the appropriate amount of  $\beta$ -CD was added to form the inclusion complex.

The temperature, speed and time of inclusion in the preparation of IC-LGZG were investigated by orthogonal test, and the inclusion method that yielded a higher content of CA was selected. Additionally, the drying temperature after inclusion was also explored, with 40 °C, 50 °C and 60 °C chosen as test points for IC-LGZG. The final preparation process was validated at laboratory, pilot and production scales. The results showed that the adaptability of the IC-LGZG preparation method across different scales, maintaining stable CA content between 79 mg/g and 92 mg/g. This stability allowed for subsequent studies on modern preparations of varying scales. Furthermore, the inclusion compounds prepared using this method were characterized via HPLC, TLC, and FT-IR. The results of HPLC confirmed the components of the aromatic water were transferred to IC-LGZG. In TLC, no yellow spot was observed in the supernatant of IC-LGZG at the corresponding position of CA, indicating successful inclusion. Conversely, the corresponding spots were observed after de-inclusion of IC-LGZG. FT-IR spectrum is obtained by detecting the absorption of infrared rays, and could be changed after the combination of  $\beta$ -CD and CA, which is an important detection form to verify the successful inclusion of CA into  $\beta$ -CD (Rajamohan et al., 2022, Rajaram et al., 2023). The spectra of IC-LGZG are roughly like those of  $\beta$ -CD, and the absorption peaks corresponding to CA are weak or disappear, which is due to the low content of CA in the IC-LGZG and the new binding with  $\beta$ -CD. These results showed that CA encapsulated into  $\beta$ -CD successfully. Considering CA's susceptibility to oxidation, and IC-LGZG is an intermediate in the production and development process of LGZG modern preparation. It was mixed with water extract powder in the stage of total mixing. The purpose of stability studies (high temperature, strong light environment and high humidity, packaged or not packaged) was to examine the factors affecting the storage conditions of the IC-LGZG. The present research results have provided the data support for the storage condition of IC-LGZG to be sealed and shady during the production process.

An ethanol-induced gastric ulcer model was chosen to verify the effectiveness of IC-LGZG and M-LGZG, while CA and ranitidine were used as controls. According to the proportion of ulcer area and H&E pathological section score, both IC-LGZG and M-LGZG effectively reduced the formation of gastric ulcer. To further confirm their mechanism of action, serum inflammatory and oxidative factors were analyzed. During the formation of gastric ulcers, various mediators undergo changes, such as increased TNF- $\alpha$  expression, a pro-inflammatory cytokine, decreased IL-10 expression, an anti-inflammatory factor, and alterations in NO content. TNF- $\alpha$  is one of the indicators to stimulate the generation of other inflammatory cytokines (Zhao et al., 2023). IL-10 as an antagonist of inflammatory could prevent macrophage activation and the generation of cytokines (Figueiredo et al., 2023). In disease conditions, excessive NO production combines with oxygen free radicals to form nitrite peroxide ions (ONOO<sup>-</sup>), leading to cellular lipids peroxidation and inflammatory damage (Wang et al., 2005). Inflammation is accompanied by oxidation, as oxygen free radicals attack polyunsaturated fatty acids in cell membranes and mitochondrial membranes, triggering lipid peroxidation, forming lipid peroxidation and further decomposing into MDA (Zhang et al., 2020). SOD is an important antioxidant that converts harmful superoxide anions into less dangerous hydroperoxides in mucous membranes. M-LGZG and IC-LGZG ameliorated the ethanol gastric ulcer-induced decreases in IL-10 and SOD and increases in TNF- $\alpha$ , NO, and MDA with the same trend as that of CA. It is speculated that CA may be the material basis of LGZG's anti-gastric ulcer effect, which regulates inflammatory and oxidation factors. Studies have indicated that CA can significantly inhibit the activity of inflammatory factors, such as the IL-8 expression in *Helicobacter pylori*-infected gastric epithelial cells by blocking the NF- $\kappa$ B pathway. Moreover, CA alleviates TNBS-induced ulcerative colitis in rats by regulating the JAK2 / STAT3 / SOCS3

pathway (Muhammad et al., 2015, Elhennawy et al., 2021), and plays an anti-inflammatory role through various signalling pathway like TLR4/MyD88 (Chen et al., 2022), JNK/p38 MAPK (Chen et al., 2023) and PI3K/AKT (Wu et al., 2020), etc, in different disease models. As point, the anti-ulcer mechanism of LGZG may be related to the above pathways.

## 5. Conclusion

In this study, we explored the delivery of the volatile component CA from LGZG decoction to solid preparation by investigating its chemical composition and pharmacological effects. We innovatively designed an inclusion process involving the direct addition of  $\beta$ -CD to aromatic water, optimizing it based on previous research. This optimized process significantly reduced the amount of  $\beta$ -CD required for the same inclusion rate and holds valuable guidance for future production endeavors (Gu et al., 2019). The process effectively transferred the volatile components from LGZG decoction to the resulting volatile components preparation. Chemical characterization and stability studies confirmed that CA was successfully incorporated into  $\beta$ -CD and demonstrating good stability. Utilizing an ethanol-induced gastric ulcer rat model, we found that the preparation did not compromise the efficacy of the volatile component or the final product, making it highly practical. In comparison to other processes of the volatile component preparation, our process offers advantages such as reduced time, straightforward operation and minimal equipment requirements. These findings provide a robust technical foundation and data support for the subsequent research and industrial production of LGZG preparations.

## Author contributions

Ling Li designed the entire study and participated in the whole experiment; Nan Wang performed the experimental work in the laboratories of preparation process and organized the data. Xiaolong Fan helped to accomplish the literature retrieval. All experiments were under the guidance of Ning He and Tong Zhang. All authors discussed and revised the manuscript.

## Funding

The authors are thankful for the financial support from the National Key Research and Development Program of China (2022YFC3501705); the National Natural Science Foundation of China general projects (82274066); the Shanghai Leading Talents Program (SHLJ2019100); the Shanghai Science and Technology Innovation Project (22S21901200); the Science and Technology Development Fund of Shanghai University of Traditional Chinese Medicine (23KFL046).

## Declaration of competing interest

The authors declare that they have no known competing financial interests or personal relationships that could have appeared to influence the work reported in this paper.

## References

- Badr, A.M., El-Orabi, N.F., Mahran, Y., et al., 2023. In vivo and In silico evidence of the protective properties of carvacrol against experimentally-induced gastric ulcer: Implication of antioxidant, anti-inflammatory, and antiapoptotic mechanisms. *Chem. Biol. Interact.* 382, 110649 <https://doi.org/10.1016/j.cbi.2023.110649>.
- Chen, L., Yuan, J., Li, H., et al., 2023. Trans-cinnamaldehyde attenuates renal ischemia/reperfusion injury through suppressing inflammation via JNK/p38 MAPK signaling pathway. *Int. Immunopharmacol.* 118, 110088 <https://doi.org/10.1016/j.intimp.2023.110088>.
- Chen, P., Zhou, J., Ruan, A., et al., 2022. Cinnamic Aldehyde, the main monomer component of Cinnamon, exhibits anti-inflammatory property in OA synovial fibroblasts via TLR4/MyD88 pathway. *J. Cell Mol. Med.* 26, 913–924. <https://doi.org/10.1111/jcmm.17148>.

- Cheng, Y., W. Sun, M. Liu, et al., 2022. Optimization of the extraction technology of volatile components from Wuyao decoction. *China Pharm.* 33, 713-717+723.
- Christaki, S., Kelesidou, R., Pargana, V., et al., 2023. Inclusion complexes of  $\beta$ -Cyclodextrin with *Salvia officinalis* bioactive compounds and their antibacterial activities. *Plants*. 12, 2518. <https://doi.org/10.3390/plants12132518>.
- Elhennawy, M.G., Abdelaleem, E.A., Zaki, A.A., et al., 2021. Cinnamaldehyde and hesperetin attenuate TNBS-induced ulcerative colitis in rats through modulation of the Jak2/STAT3/SOCS3 pathway. *J. Biochem. Mol. Toxicol.* 35, e22730. <https://doi.org/10.1002/jbt.22730>.
- Figueiredo, F.F., Damazo, A.S., Arunachalam, K., et al., 2023. Evaluation of the gastroprotective and ulcer healing properties by *Fridericia chica* (Bonpl.) L.G. Lohmann hydroethanolic extract of leaves. *J. Ethnopharmacol.* 309, 116338 <https://doi.org/10.1016/j.jep.2023.116338>.
- Fu, C., 2008. Pharmaceutical excipients. China Press Tra Chin Med, Beijing.
- Gu, S., 2020. Study on the material standard and compound preparation of Lingguizhugan Decoction. Master. Shanghai Univ Tra Chin Med.
- Gu, S., Li, N., Li, L., et al., 2019. Optimization of  $\beta$ -cyclodextrin inclusion process for volatile constituents in Supplemented Lingui Zhugan Decoction. *Chin Trad Patent Med.* 41, 2039-2043.
- Jia, W., He, X., Jin, W., et al., 2023. *Ramulus Cinnamomi essential* oil exerts an anti-inflammatory effect on RAW264.7 cells through N-acyl ethanolamine acid amidase inhibition. *J. Ethnopharmacol.* 116747 <https://doi.org/10.1016/j.jep.2023.116747>.
- Jiang, L., Xia, N., Wang, F., et al., 2022. Preparation and characterization of curcumin/ $\beta$ -cyclodextrin nanoparticles by nanoprecipitation to improve the stability and bioavailability of curcumin. *LWT - Food Sci. Technol.* 171, 114149. doi: 10.1016/j.lwt.2022.114149.
- Li, Q., Cao, J., Tang, T., et al., 2022. Study on the value transmission of the key quality component groups of the material standard of the classical famous prescription Wenjing decoction. *Lishizhen Med. Mat. Medica Res.* 33, 873-878.
- Li, L., Du, Y., Wang, Y., et al., 2022. Atractylone Alleviates Ethanol-Induced Gastric Ulcer in Rat with Altered Gut Microbiota and Metabolites. *J. Inflamm.* 15, 4709-4723. <https://doi.org/10.2147/JIR.S372389>.
- Li, C., Zhang, J., Zhang, H., et al., 2016. Study on  $\beta$ -cyclodextrin inclusion Process of Volatile oil from Atractylodes Rhizome and *Ramulus Cinnamomi* from Tingli Shengmai decoction. *Lishizhen Med Mat Medica Res.* 27, 2167-2170.
- Liu, R., Gou, L., Yu, L., et al., 2013. The effects of the volatile oil of *Ramulus Cinnamomi* and cinnamaldehyde on death protection rate in H1N1-infected mice and mechanism of TLR/IFN signal pathway. *Pharma Clin. Chin. Mat Medica.* 29, 33-36. <https://doi.org/10.13412/j.cnki.zyy1.2013.04.050>.
- Liu, J., Zhang, Q., Li, R.L., et al., 2020. The traditional uses, phytochemistry, pharmacology and toxicology of *Cinnamomi ramulus*: a review. *J. Pharm. Pharmacol.* 72, 319-342. <https://doi.org/10.1111/jphp.13189>.
- Luo, Y., Yang, M., Li, S., et al., 2016. Explore scientific connotation of "taking when fragrances volatilized fiercely" for Yinqiao powder based on dynamic changes in contents of volatile components in decoction. *China J. Chin Materia Medica.* 41, 3349-3354. <https://doi.org/10.4268/cjmm.20161807>.
- Mic, M., Pîrnău, A., Floare, C.G., et al., 2023. Inclusion of a catechol-derived Hydrzinyli-Thiazole (CHT) in  $\beta$ -Cyclodextrin nanocavity and its effect on antioxidant activity: a calorimetric, spectroscopic and molecular docking approach. *Antioxidants*. 12, 1367. <https://doi.org/10.3390/antiox12071367>.
- Muhammad, J.S., Zaidi, S.F., Shaharyar, S., et al., 2015. Anti-inflammatory effect of cinnamaldehyde in *Helicobacter pylori* induced gastric inflammation. *Biol. Pharm. Bull.* 38, 109-115. <https://doi.org/10.1248/bpb.b14-00609>.
- Niu, W., 2022. Preparation, characterization and the therapeutic efficacy against ulcerative colitis of baicalein-cyclodextrin inclusion. Master. Nanjing Univ Chin Med.
- Qiang, J., Ye, B., Lin, L., et al., 2014. Study of stability influence factors of eugenol and cinnamaldehyde with different existence state. *Trad. Chin Drug Res. Clin. Pharmacol.* 25, 89-92. <https://doi.org/10.3969/j.issn.1003-9783.2014.01.024>.
- Rajamohan, R., Mohandoss, S., Ashokkumar, S., et al., 2022. A novel and water-soluble material for coronavirus inactivation from oseltamivir in the cavity of methyl and sulfated- $\beta$ -cyclodextrins through inclusion complexation. *J. Pharm. Biomed. Anal.* 221, 115057 <https://doi.org/10.1016/j.jpba.2022.115057>.
- Rajaram, R., Lee, Y.R., Angaiha, S., 2023. Supramolecular assembly of benzocaine bearing cyclodextrin cavity via host-guest complexes on polyacrylonitrile as an electrospun nanofiber. *J. Pharm. Biomed. Anal.* 225, 115223 <https://doi.org/10.1016/j.jpba.2022.115223>.
- Su, Z., Qin, Y., Zhang, K., et al., 2019. Inclusion complex of exocarpium citri grandis essential oil with  $\beta$ -Cyclodextrin: characterization, stability, and antioxidant activity. *J. Food Sci.* 84, 1592-1599. <https://doi.org/10.1111/1750-3841.14623>.
- Wang, Y., 2012. Treatment of 50 cases of gastric epigastric pain with Linggui Zhugan Decoction. *Shaanxi J. Tra Chin Med.* 33, 523-525.
- Wang, L., Shi, G.G., Yao, J.C., et al., 2005. Expression of endothelial nitric oxide synthase correlates with the angiogenic phenotype of and predicts poor prognosis in human gastric cancer. *Gastric Cancer* 8, 18-28. <https://doi.org/10.1007/s10120-004-0310-7>.
- Wang, Q., Zheng, X., Wu, F., et al., 2022. Research progress on the application of volatile oil in oral preparations of traditional Chinese medicine. *Chin Trad Patent Med.* 44, 498-503. <https://doi.org/10.3969/j.issn.1001-1528.2022.02.030>.
- Wu, J.R., Zhong, W.J., Chen, Z.D., et al., 2020. The protective impact of Trans-Cinnamaldehyde (TCA) against the IL-1 $\beta$  induced inflammation in *in vitro* osteoarthritis model by regulating PI3K/AKT pathways. *Folia Histochem. Cytobiol.* 58, 264-271. <https://doi.org/10.5603/FHC.a2020.0025>.
- Xiang, C., Zhang, J., Li, J., et al., 2017. Preparation and Evaluation of Rhizoma Atractylodis macrocephalae and *Ramulus cinnamomi* Oil- $\beta$ -cyclodextrin Inclusion Complex. *Nat. Prod. Res. Dev.* 29, 46-51. <https://doi.org/10.16333/j.1001-6880.2017.1.008>.
- Xie, Y., 2017. A Study on the Law of Medication for Stomachache as Followed by the Medical Practitioners in the Period of the Song, Jin and Yuan Dynasties. Doctor, Guangzhou Univ Chin Med.
- Xu, F., Wang, D., Wang, F., et al., 2016. Research progress on pharmacological effects of *Rimulus cinnamomi* essential oil. *China J Tra Chin Med Pharm.* 31, 4653-4657.
- Ye, Z., 2016. Effect of Linggui Zhugan Decoction in treating 60 cases of gastric epigastric pain. *For All Health.* 10, 134-135.
- Yi, Y., Chen, Z., 2006. Evaluation of cyclodextrin inclusion of the volatile components in compound traditional Chinese medicine. *J. South Med. Univ.* 26, 1337-1340.
- Zhang, Z., 2006. Synopsis of Golden Chamber. China Press Tra Chin Med, Beijing.
- Zhang, S., Wang, H., Li, Q., 2011. Guideline for the management of epigastric pain. *Chin Med Modern Distance Edu China.* 9, 127-129.
- Zhang, G., Zhang, M., Tan, L., 2020. Study on anti-inflammatory effect and mechanism of Shenju lotion. *J Xinjiang Med Univ.* 43, 1236-1240.
- Zhang, Y., 2019. Literature Research and Data Mining Based on Epigastralgia Medical Cases of Famous Ancient Scholars. Master, Zhejiang Chin Med Univ.
- Zhao, Y., Cheng, G., Gao, Y., et al., 2023. Green synthetic natural carbon dots derived from *Fuligo Plantae* with inhibitory effect against alcoholic gastric ulcer. *Front. Mol. Biosci.* 10, 1223621. <https://doi.org/10.3389/fmol.2023.1223621>.